Influence of Peripheral Hydrogen Bonding on the Mechanical Properties of Photo-Cross-Linked Star-Shaped Poly(d , l -lactide) Networks

ARTICLE *in* BIOMACROMOLECULES · SEPTEMBER 2005

Impact Factor: 5.75 · DOI: 10.1021/bm050375i · Source: PubMed

4 AUTHORS, INCLUDING:

Afia Karikari
Dow Chemical Company
7 PUBLICATIONS **177** CITATIONS

SEE PROFILE

Influence of Peripheral Hydrogen Bonding on the Mechanical Properties of Photo-Cross-Linked Star-Shaped Poly(D,L-lactide) Networks

Afia S. Karikari,[†] Wesleigh F. Edwards,[†] Jeffrey B. Mecham,[‡] and Timothy E. Long*[,†]

Department of Chemistry, Macromolecules and Interfaces Institute, Virginia Polytechnic Institute and State University, Blacksburg, Virginia 24061, and NanoSonic, Inc., 1425 South Main Street SE, Blacksburg, Virginia 24060

Received June 3, 2005; Revised Manuscript Received July 19, 2005

Four-arm, star-shaped poly(D,L-lactide) (PDLLA) oligomers of controlled molar mass and narrow molar mass distribution were successfully synthesized by use of an ethoxylated pentaerythritol initiator. Derivatization of the terminal hydroxyl groups with either methacrylic anhydride (MAAH) or 2-isocyanatoethyl methacrylate (IEM) to yield PDLLA-M (M = methacrylate end group) and PDLLA-UM (UM = urethane methacrylate end group), respectively, was monitored by in situ Fourier transform infrared (FTIR) spectroscopy. Photo-cross-linking of the functional oligomers yielded networks with high gel contents (>95%). The glass transition temperature (T_g) of these networks was strongly dependent on prepolymer molar mass, and networks based on low molar mass precursors were more rigid than the networks obtained from higher molar mass oligomers. The tensile strength (TS) and Young's modulus of the PDLLA-M samples, approximately 7 and 17 MPa, respectively, were significantly lower than the values of 19 MPa (TS) and 113−354 MPa (Young's modulus) for the PDLLA-UM samples. The introduction of terminal hydrogen-bonding sites that were adjacent to the photo-cross-linking site resulted in higher performance poly(lactide)-based bioadhesives.

Introduction

Biodegradable polyesters, such as poly(lactides) (PLA) and poly(glycolides), are widely utilized in a variety of biomedical applications including surgical fixation devices and controlled drug delivery.[1,2] The use of lactide-based polymers as bioadhesives for human tissue is emerging as a preferred alternative to suturing.[3] An ideal bioadhesive must have adequate viscosity prior to application, adhere to the tissue substrates, and cure rapidly. Additionally, the adhesive should biodegrade without eliciting local or systematic toxicity and must provide strong and complete closure throughout the healing process.[4]

Current approved clinical adhesives include alkyl cyanoacrylates,[5] gelatin−resorcinol−formaldehyde (GRF) glue,[6−8] and fibrin glue.[9,10] Alkyl cyanoacrylates cure rapidly and form strong tissue interfaces with high bond strengths of 1−3 MPa.[11−13] However, the toxicity of the degradation product, formaldehyde,[14] which results in tissue damage and elicits dose-dependent carcinogenicity,[11,15−17] restricts alkyl cyanoacrylates to topical skin use. The tensile strengths of the GRF and fibrin glues (0.050−0.170 MPa[12,18] and 0.002−0.040 MPa,[12,19] respectively) are inferior to that of alkyl cyanoacrylates and are therefore inadequate for bonding with high tensile loads.[11,20,21] In addition, fibrin glue is produced from human serum and is not commercially viable, while GRF glue has formaldehyde as a reactant and associated toxicity issues.[22]

Efforts to develop nontoxic bioadhesives with high mechanical properties thus continue, and the exploitation of biodegradable and biocompatible polymeric materials as tissue adhesive candidates are hence generating considerable interest.[23−36] The use of polymeric bioadhesives in clinical applications is especially advantageous in cross-linking techniques[25,26] such as laser-assisted vascular repair. Also known as tissue soldering, the process involves the laser-induced bonding of tissue surfaces with a bioadhesive.[27] Tissue soldering is particularly desired in surgical anastomosis in cardiac bypass and limb and digit reattachment surgery where multiple anastomoses are typically required. Poly(L-lactic-*co*-glycolic acid) scaffolds doped with the traditional protein solder mix of porcine serum albumin and indocyanine green dye were studied extensively for laser-assisted vascular repair.[28−30] The optimal temperature for tissue soldering in most of these systems is reportedly around 65 °C[31] and such a high temperature can result in thermal damage of neighboring tissues. As a consequence, there is the need for low T_g tissue adhesives that cure rapidly at relatively low temperatures and exhibit high mechanical strength.[32]

Polymeric bioadhesives with pendant photofunctional groups are advantageous because they are curable by use of ultraviolet (UV) or visible light, cure quickly at physiological temperature or 37 °C, and produce minimal heat during

* Corresponding author: telephone +1-540-231-2480; fax +1-540-231-8517; e-mail telong@vt.edu.
[†] Virginia Polytechnic Institute and State University.
[‡] NanoSonic, Inc.

10.1021/bm050375i CCC: $30.25
Published on Web 08/19/2005

photopolymerization.[33] Ono et al.[34] synthesized a cationic polymeric bioadhesive based on chitosan, a polysaccharide, with azide and lactose moieties. However, the mechanical strength of the photo-cross-linked chitosan hydrogels was comparable to that of fibrin glue. Matsuda and co-workers[35,36] have used photoinduced polymerization to prepare tissue adhesives based on photoreactive gelatin and diacrylated poly(ethylene glycol) (PEG) macromonomers. In our laboratories,[37] we have also demonstrated the photoreversibility of coumarin containing PEG monols and diols, and PEG resistance to protein adhesion in biomedical applications is widely reported.

Studies on photo-cross-linking of star-shaped polymers based on PLA and other biodegradable polyesters have mainly concentrated on their use in composites and as matrixes for drug delivery and scaffolds in tissue engineering,[38−40] with only a few applicable for use as bioadhesives.[41] This is attributed to generally brittle polymers with high moduli at physiological temperatures, thus limiting their use as tissue adhesives. Helminen et al.[39] initiated D,L-lactide (DLLA) with pentaerythritol and subsequently functionalized the hydroxyl end groups with methacrylic anhydride (MAAH). The methacrylated polymers were thermally cross-linked at 90 °C for 24 h to obtain highly cross-linked networks; a high temperature was required due to the relatively high T_g of the functionalized oligomer, resulting in unsuitable bioadhesives. To photo-cross-link at physiological temperature, 30 wt % of a reactive monomer such as dimethacrylated butanediol was added as a diluent to the functionalized oligomers.

To achieve well-defined, photoreactive star poly(D,L-lactide) (PDLLA) bioadhesives that are suitable for potential use in laser-assisted vascular repair, we have in the present work synthesized oligomeric four-arm, star-shaped PDLLAs with methacrylate terminal groups (PDLLA-M). The four-arm star PDLLAs were synthesized by use of a pentaerythritol ethoxylate initiator in order to take advantage of the biocompatible, nontoxic, nonimmunogenic, and water-soluble ethylene oxide units.[33] Efforts to lower the T_g of PLA have involved the use of biocompatible plasticizers such as the lactide monomer,[42] supercritical carbon dioxide,[43] polysaccharides,[44] poly(ϵ-caprolactone),[45] and polyisoprene.[46] Another well-known plasticizer for PLA is PEG.[47−50] However, Mccarthy and co-workers[50] have shown that blends of PLA with PEG contents higher than 50 wt % resulted in undesirable highly crystalline blends. In a related study to circumvent crystallinity and decrease migration and hydrophilicity, Hillmyer and co-workers[51] reported the synthesis of a perfectly alternating copolymer of lactic acid and ethylene oxide. Blending of PLA and the alternating copolymer resulted in effective plasticization of the PLA. On the basis of these earlier PEG plasticizer efforts, the oligomeric PEG-based multifunctional initiator was used to obtain low molar mass, star-shaped PDLLAs with low T_gs that were suitable for application as a viscous liquid prior to photo-cross-linking. Previous efforts in our laboratories have also focused on the incorporation of various hydrogen-bonding groups into linear and star-shaped polymers in order to probe influence on rheological, thermal, and mechanical properties.[52−56] In the present work, the influence of telechelic urethane hydrogen bonding on potential PDLLA bioadhesives was probed via functionalization with isocyanatoethyl methacrylate (IEM). ^{1}H NMR spectroscopy and size-exclusion chromatography (SEC) were used to characterize the PDLLA stars, and in situ Fourier transform infrared (FTIR) spectroscopy was used to monitor the functionalization of the star oligomers with IEM. Tensile testing and dynamic mechanical analysis (DMA) were used to evaluate the mechanical properties of free-standing, thin photo-cross-linked films.

Experimental Section

Materials. D,L-Lactide (DLLA, 98%) from Aldrich was recrystallized twice from ethyl acetate and dried for several days in vacuo at 40 °C prior to use. Pentaerythritol ethoxylate (EO/OH 15/4, Aldrich) was dried in vacuo at 60 °C for 24 h. Stannous(II) ethylhexanoate ($Sn(Oct)_2$, Aldrich) was used as received. Toluene (99.5%, EMD Chemicals) and tetrahydrofuran (THF, 99.98, EMD Chemicals) were distilled from metallic sodium and benzophenone (99%, Aldrich)/tetra(ethylene glycol) dimethyl ether (99%, Aldrich) immediately prior to use. Methacrylic anhydride (MAAH, 94%, Aldrich), 2-isocyanatoethyl methacrylate, (IEM, 98%, Aldrich), and dibutyltin dilaurate (DBT-12, 95%, Aldrich) were used without further purification.

Synthesis of 4-Arm Star-Shaped PDLLA Oligomers. DLLA (5 g, 0.035 mol) was added under nitrogen to a flame-dried, 50-mL round-bottomed flask containing a magnetic stir bar and sealed with a rubber septum. The system was purged with nitrogen. Pentaerythritol ethoxylate (2.7 g, 0.0033 mol) was added via syringe under nitrogen. The reaction flask was immersed in a 130 °C oil bath and sufficient time was allowed for the lactide to melt. A catalytic amount of $Sn(Oct)_2$ (0.0006 mol $\approx$ 200 ppm) in toluene was added, and the reaction mixture was allowed to stir for 10 min. The reaction temperature was decreased to 120 °C, and the reaction was allowed to proceed for 24 h. The product was dissolved in chloroform, precipitated several times in a hexane/methanol mixture (90:10), and dried in vacuo at 60 °C for 24 h.

Functionalization of Star PDLLA with MAAH. The star PDLLA (5 g) was added to a flame-dried, two-neck round-bottomed flask equipped with a magnetic stir bar and a water condenser. Freshly distilled toluene (30 mL) was added to the flask to prepare a 16 wt % polymer solution, and the solution was allowed to stir. After 10 min, 5-fold excess of MAAH (6.8 g, 0.044 mol) was added via syringe. The mixture was heated to reflux under nitrogen for 5 h. The product was precipitated several times in hexane and dried under vacuum at room temperature for at least 24 h. Quantitative functionalization was confirmed by ^{1}H NMR spectroscopy.

Functionalization of Star PDLLA with IEM. Star PDLLA (5 g) was weighed into a septum-sealed two-neck, round-bottomed flask with a stir bar. The flask was equipped with a water condenser and placed in a 70 °C oil bath. THF (30 mL) was added under nitrogen to make a 16 wt %

polymer solution. IEM (1.5 g, 0.0097 mol) was syringed into the reaction mixture under nitrogen upon polymer dissolution. The mixture was stirred for 10 min and a catalytic amount of DBT-12 was added. The reaction was allowed to run for 1 h. The precipitate was isolated in hexane and dried in vacuo for at least 24 h. Quantitative functionalization was confirmed by ^{1}H NMR spectroscopy.

Photo-Cross-Linking. The methacrylate-functionalized star polymer (0.5 g) and 0.02 g (4 wt %) of 2,2-dimethyl-2-phenylacetophenone (DMPA, Aldrich) were dissolved in 1.0 mL of chloroform as a 25 wt % solution. The mixture was stirred until it was homogeneous and poured into clean poly(tetrafluoroethylene) molds. The molds were stored overnight at room temperature in the absence of light to evaporate the chloroform. The molds were passed through a Fusion UV system (model LC-6B benchtop conveyor) at 5 ft/min to achieve an energy dose of 1.63 J/cm^2 (UVA) resulting in photo-cross-linking to form uniform films. The irradiance and energy density were measured with an EIT UV Power Puck radiometer. Soxhlet extraction was performed on the cross-linked film for 12 h and the gel fraction of the dry films was determined gravimetrically.

Characterization: (A) Nuclear Magnetic Resonance Spectroscopy. The polymer composition, number-average molar mass, and percent functionalization were determined by ^{1}H NMR spectroscopy. The spectra were obtained on a Varian Unity spectrometer operating at 400 MHz with $CDCl_3$ as the solvent.

(B) Size-Exclusion Chromatography. Molar masses and molar mass distributions were determined at 40 °C in THF (ACS grade) at a flow rate of 1 mL/min by use of a Waters 717 Autosampler equipped with a Waters 2410 refractive index detector, a Wyatt Technology MiniDAWN multiangle laser light scattering (MALLS) detector, and a Viscotek 270 viscosity detector. Reported molar masses are based on absolute measurements using the MALLS detector.

(C) Differential Scanning Calorimetry. Glass transition temperatures were determined under nitrogen on a Perkin-Elmer Pyris 1 cryogenic instrument at a heating rate of 10 °C/min. The T_g is reported as the transition midpoint during the second heat.

(D) In Situ FTIR Spectroscopy. In situ FTIR spectroscopic analysis was performed on an ASI React IR 1000 (ASI Applied Systems Inc.) attenuated total reflectance (ATR) spectrometer. Our laboratories have demonstrated the efficacy of in situ FTIR spectroscopy for diverse organic reactions and polymerization processes.[57−63]

(E) Tensile Testing. Tensile analysis was conducted with an Instron Model 5500 universal tester at room temperature with a cross-head speed of 10 mm/min and an initial grip separation of 16 mm. Five dog-bone microtensile test specimens were punched from the photo-cross-linked star oligomer films with an average thickness of 26 μm with a standard die (ASTM D3368). Five specimens were tested and the average values are reported.

(F) Dynamic Mechanical Analysis. DMA was performed on a TA Instruments DMA Q800 at 5 °C/min and 1 Hz. The film geometry was in tension mode. T_g is reported as the temperature corresponding to the maximum in the loss modulus versus temperature curve.

Results and Discussion

Polymerization. Four-arm, star-shaped, PDLLAs were prepared by use of pentaerythritol ethoxylate to initiate the ring-opening polymerization of DLLA as depicted in Scheme 1. The initiator, PTOLEO, was previously used to prepare spirocyclic tin initiators[64−66] in the synthesis of well-defined, high molar mass, star polylactones with narrow molar mass distributions. In the present work, PTOLEO was used without conversion to the spirocyclic tin initiator. ^{1}H NMR was used to characterize the PTOLEO and the presence of 15 ethylene oxide units and four hydroxyl groups was confirmed. Well-defined, four-arm star-shaped oligomers with narrow molar mass distribution (1.06−1.20) were prepared over a molar mass range of 1500−9500 g/mol (Table 1).

^{1}H NMR spectroscopy was used to characterize the star PDLLAs (Figure 1). Resonance a, which was assigned to the methine proton in the PDLLA repeat unit at 5.12 ppm, and resonance h at 3.41 ppm, which was assigned to the β-methylene protons of the ethylene oxide unit adjacent to the DLLA repeat units, were compared to obtain the absolute number-average molar mass.[66] It was assumed that each initiator resulted in the growth of exactly four PDLLA chains and arms of nearly equivalent molar mass were obtained. Excellent agreement existed between the ^{1}H NMR and SEC number-average molar mass, and the measured molar mass was in agreement with the targeted molar mass based on the assumption of four equally reactive hydroxyls in the initiator. PTOLEO was an effective initiator for low molar mass PDLLA oligomers but was ineffective in the polymerization of higher molar mass stars, presumably due to transesterification reactions.[67,68] This limitation was acceptable for our studies since the objective was to prepare low-viscosity oligomeric precursors for subsequent network formation.

The T_g of the four-arm star PDLLA increased from −29 to 27 °C as the molar mass was increased from 1500 to 9500 g/mol (Table 1). The increase in T_g corresponded linearly with the weight fraction of oligo(ethylene oxide) (EO) initiator fragments to PDLLA segments. The lower molar mass star-shaped polymers had shorter PLA segments and higher EO compositions, which contributed to lower T_gs. As the PDLLA segment length increased with increasing star molar mass, the weight percent of EO in the polymer decreased, thereby increasing the T_g. In addition, the glass transition temperature of PDLLA segments also increased with an increase in molar mass; however, the decoupling of the influence of EO composition and final molar mass was not conducted.

Modification. Star-shaped oligomers with a range of molar masses were modified with either MAAH or IEM to introduce terminal photoreactive methacrylate sites (Scheme 1). MAAH and IEM were quantitatively reacted with the terminal hydroxyl groups in solution to produce photoreactive four-arm star-shaped oligomers with methacrylate end groups (PDLLA-M) and with methacrylate end groups with an

Scheme 1. Synthetic Methodology for the Preparation of Four-Arm, Star-Shaped PDLLA, Functionalization,[a] and Subsequent Photo-Cross-Linking

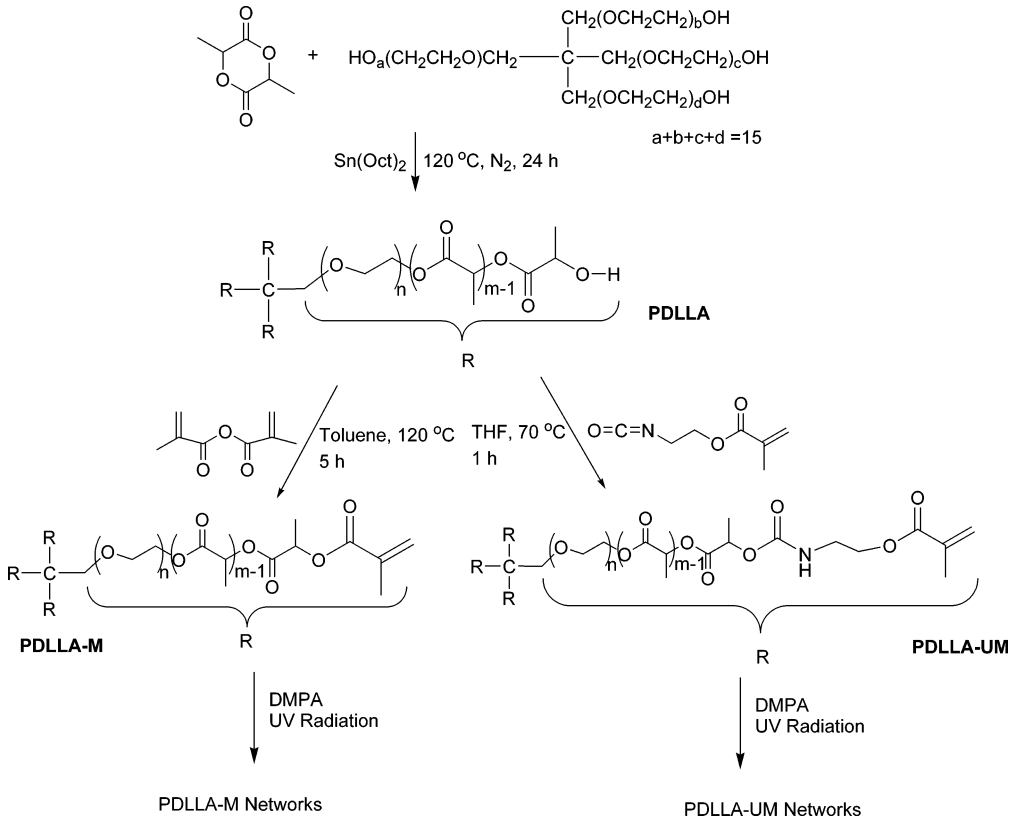

[a] Functionalization with MAAH produces PDLLA-M; functionalization with IEM produces PDLLA-UM,

Table 1. Characterization of Four-Arm Star-Shaped PDLLA Oligomers

M_n (target) (g/mol)	M_n[a] (g/mol)	M_n[b] (g/mol)	M_w/M_n	yield (%)	EO[c] (wt %)	T_g[d] (°C)
1500	1540	1510	1.08	97	54	−29
2300	2270	2270	1.07	100	26	−16
2300	2300	2870	1.06	96	23	−10
3000	3540	3160	1.07	97	8.6	−1
5800	6620	5330	1.20	93	4.0	11
10 800	7700	7840	1.15	88	1.6	22
10 800	7930	8050	1.09	79	1.5	23
10 800	10 400	9510	1.11	90	0.8	27

[a] ^{1}H NMR in $CDCl_3$. [b] SEC using an absolute MALLS detector. [c] Weight % ethylene oxide units calculated using ^{1}H NMR spectroscopy. [d] DSC under nitrogen at 10 °C/min (second heating).

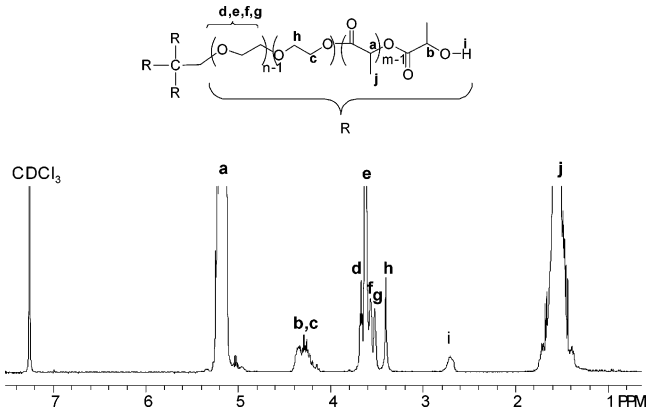

Figure 1. ^{1}H NMR spectrum of a typical four-arm star-shaped PDLLA.

adjacent urethane segment (PDLLA-UM). The urethane moiety was incorporated to provide hydrogen-bonding interactions and potentially improve the mechanical properties of the final photo-cross-linked networks. Previously, Hsu and Lin[69] demonstrated the superior biocompatibility of polyurethanes based on poly(hexylethyl carbonate). Polyurethanes are also widely utilized in a variety of biomedical applications including vascular prosthesis.[70] Furthermore, IEM-based polyurethanes[32,71] were prepared earlier for the preparation of materials for various biomedical applications, and it was presumed that their incorporation at low levels would not significantly influence cytotoxicity.

^{1}H NMR and FTIR spectroscopies were used to ensure quantitative conversion of terminal hydroxyl groups to methacrylate functionality (Figure 2). The ^{1}H NMR spectrum of PDLLA-UM (Figure 2) exhibited three additional resonances, n, o, and p, that were not observed in the spectrum for PDLLA-M, and these were attributed to the urethane segment. The resonance at 3.58 ppm corresponded to the methylene proton that is adjacent to the methacrylate site.

^{1}H NMR number-average molar mass determinations for PDLLA-M were performed in a fashion similar to the analysis of the hydroxyl-terminated PDLLA stars. A comparison of the integration of the resonance at 3.41 ppm with integrations for resonances m and l, which were assigned to the olefinic protons of PDLLA-M at 6.19 and 5.63 ppm, respectively, and the resonance from the methyls of the methacrylate end group at 1.96 ppm indicated the percent functionalization. The extent of functionalization that was typically obtained with MAAH was 90−98%. Comparison

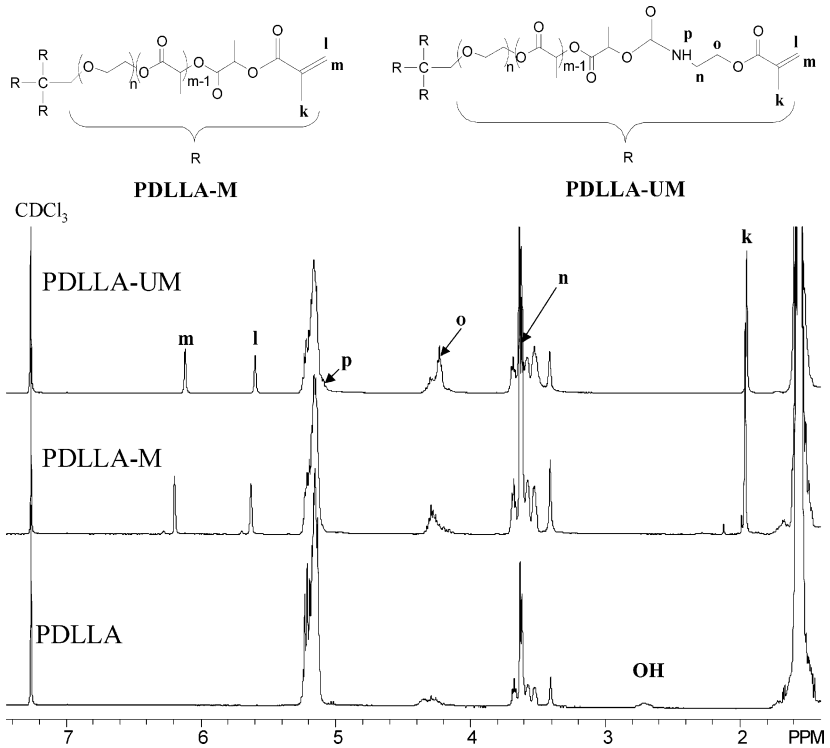

Figure 2. Comparison of the ^{1}H NMR spectra of star-shaped PDLLA, PDLLA-M, and PDLLA-UM.

of the resonance at 3.41 ppm with the signals from resonances m and l, which were assigned to the olefinic protons of PDLLA-UM at 6.12 and 5.61 ppm, respectively, and with the methyl assigned to the protons of the methacrylate group at 1.95 ppm indicated quantitative end group functionalization (>98%).

The urethane resonance (o) overlapped with the methylene protons of the EO segment, which was adjacent to the lactide main chain. Last, resonance p, which overlapped with the methine resonance of the lactide main chain, corresponded to the N−H of the urethane linkage.[71]

In Situ FTIR Monitoring. In situ FTIR spectroscopy was used to monitor the reaction between IEM and PDLLA (Figure 3). As expected on the basis of our earlier efforts, the well-resolved isocyanate absorbance disappeared and a strong carbonyl absorbance appeared.[72] In addition, the consumption of the hydroxyl group and the concurrent growth of the NH stretch are depicted in Figure 3a. The hydroxyls were completely reacted within the first hour of the reaction and the NH absorbance increased steadily as the hydroxyls were consumed and remained subsequently constant.

A significant amount of the isocyanate reacted in the first 6 min and gradually reached a constant absorbance within 1 h (Figure 3b). The constant absorbance after complete hydroxyl consumption was attributed to an intentional slight excess of isocyanate. The formation of the urethane carbonyl absorbance at 1725 cm^{-1} (Figure 3c) increased rapidly within the first 30 min and remained constant in a similar manner. It is noted that the carbonyl absorbance at 1775 cm^{-1}, which was attributed to the ester carbonyl group of PDLLA, remained constant throughout the entire reaction. The analysis therefore indicated that the formation of PDLLA-UM was rapid, and quantitative conversion of the hydroxyl end groups was achieved in less than 40 min. A similar in situ FTIR spectroscopic analysis was attempted for the MAAH functionalization reaction; however, a large excess of the anhydride was required, and thus the OH and methacrylate carbonyl absorbances were relatively weak and not reliable for spectroscopic analysis.

The FTIR spectra of star PDLLA, PDLLA-M, and PDLLA-UM after precipitation and drying (Figure 4) further confirmed the disappearance of the OH absorbance for both PDLLA-M and PDLLA-UM (Figure 4B). The NH stretch that resulted from the urethane NH for PDLLA-UM was clearly observed at 3400 cm^{-1} and the carbonyl absorbance for PDLLA-UM was broadened, which was consistent with the incorporation of a urethane carbonyl in addition to the new methacrylate carbonyl (Figure 4C). Furthermore, the alkene C═C stretch was detected in Figure 4D for both PDLLA-M and PDLLA-UM at 1640 cm^{-1}.

Photo-Cross-Linking and Thermal Analysis. Recently, Lin-Gibson et al.[71] studied the properties of linear PEG hydrogels functionalized with MAAH and IEM. The urethane spacer was incorporated in order to probe the influence of adjacent hydrogen bonding on the mechanical properties of the resulting network. However, the influences of the urethane segment and topology in the photo-cross-linked network on the thermal and mechanical properties were not described. The authors focused on the shear moduli of only the hydrogels that were prepared from MAAH-functionalized PEG and utilized only rheological and uniaxial compression measurements. In the present work, detailed thermal and mechanical analyses of the networks of PDLLA-M and PDLLA-UM were conducted. In addition, the influence of precursor molar mass and end group composition on the mechanical properties was investigated. The photo-cross-linking of star PDLLA-M and PDLLA-UM was accom-

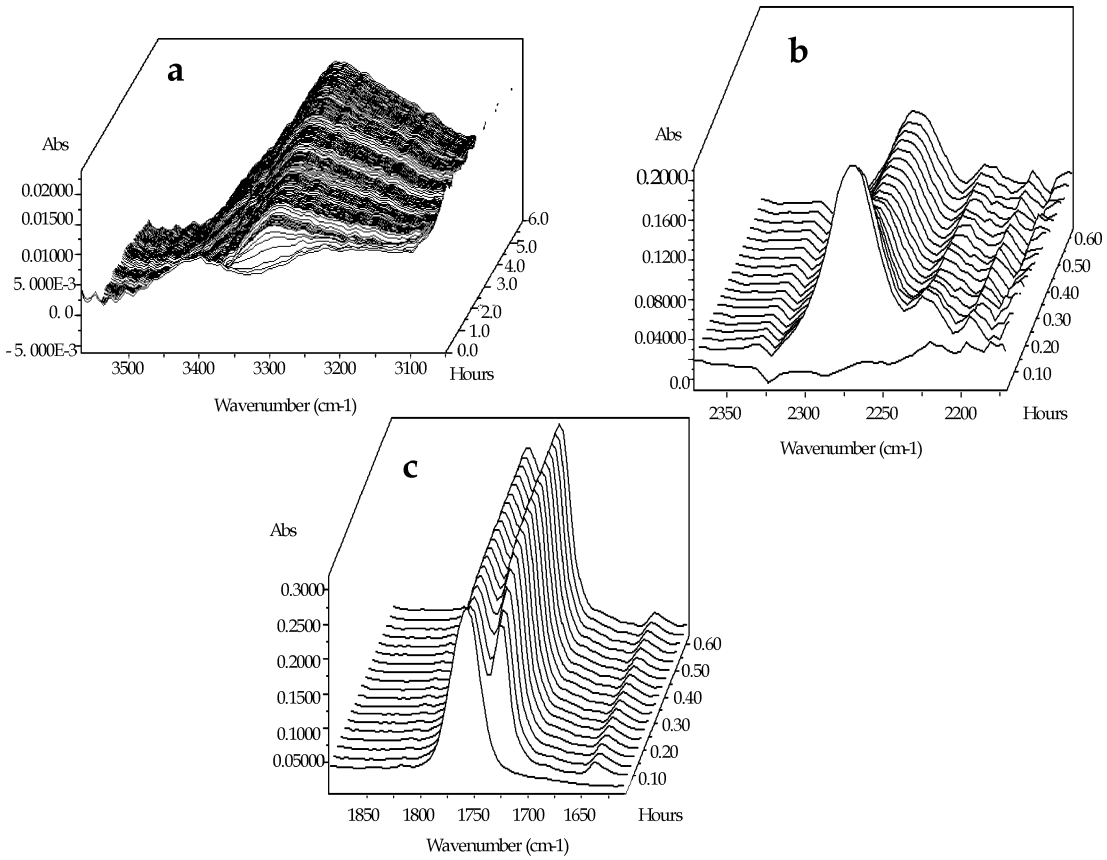

Figure 3. Waterfall FTIR spectra of the functionalization of star PDLLA with IEM showing (a) OH/NH region, (b) isocyanate region, and (c) C═C region.

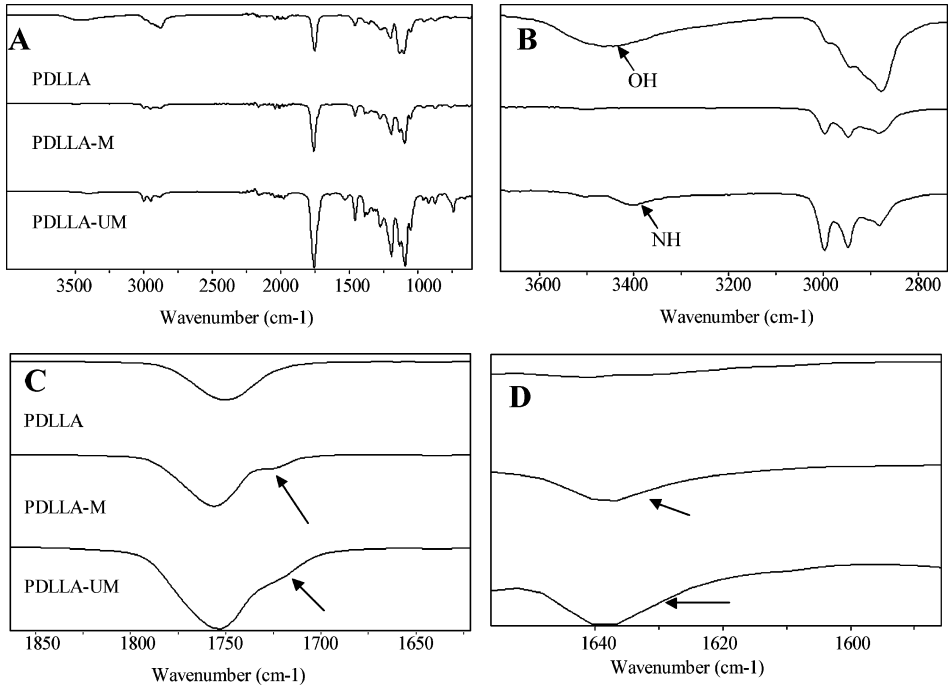

Figure 4. Stacked FTIR spectra of star PDLLA, PDLLA-M, and PDLLA-UM: (A) full spectra; (B) OH/NH region; (C) C═O region; (D) C═C region.

plished with DMPA as the photoinitiator (Scheme 1). High gel contents (94−99%) were obtained; however, as expected, the gel fractions were slightly lower for the higher molar mass precursors in accordance with literature.[33,40] The effect of precursor molar mass on the final gel content was attributed to the higher concentration of photofunctional end groups in the low molar mass precursors. The temperature of the film surfaces measured with a Raytek portable infrared thermometer ranged from 25 to 30 °C. This slight increase in reaction temperature was primarily attributed to infrared heating during photo-cross-linking; however, the exothermic conversion of π-bonds in the methacrylic groups to σ-bonds

Table 2. Thermal Properties of Photo-Cross-Linked Networks of PDLLA-M and PDLLA-UM

backbone	M_n[a] prepolymer (g/mol)	gel content (%)	T_g[b] prepolymer (°C)	T_g[b] network (°C)	T_g[c] network (°C)
PDLLA-M	2890	97	−10	20	55
PDLLA-M	7930	95	23	24	37
PDLLA-M	9510	90	27	27	
PDLLA-UM	2270	99	−16	27	54
PDLLA-UM	7840	94	22	25	33

[a] SEC, MALLS with polystyrene standards. [b] DSC at 10 °C/min. [c] DMA at 5 °C/min.

Table 3. Tensile Properties of Photo-Cross-Linked PDLLA-M and PDLLA-U Networks

backbone	M_n[a] prepolymer (g/mol)	gel content (%)	tensile strength (MPa)	tensile modulus (MPa)	elongation at break (%)
PDLLA-M	2870	97	8 ± 1	21 ± 10	43 ± 5
PDLLA-M	9510	90	7 ± 3	12 ± 4	172 ± 9
PDLLA-UM	2270	99	21 ± 3	354 ± 42	44 ± 4
PDLLA-UM	7840	94	17 ± 3	113 ± 13	138 ± 8

was also expected to contribute. There was no attempt to elucidate the contribution from both sources, and the overall temperature rise reflects a combination of these two mechanisms. The low molar mass precursors had lower T_gs, which facilitated diffusion during the photo-cross-linking reaction compared to the high molar mass precursors with $T_g = 22-23$ °C (Table 2). It was reasonable to assume that the increased chain mobility would lead to a higher degree of cross-linking and increased gel content. The results indicated that during the photo-cross-linking reaction, the T_g of the networks approached room temperature and stopped once it reached the reaction temperature.

The cross-linked samples exhibited higher T_gs than the corresponding non-cross-linked precursors, and the T_g increase upon photo-cross-linking was greater with the low molar mass precursors (Table 2). As expected, the T_gs obtained by DMA were notably higher than the DSC values due to the greater sensitivity and frequency dependency of DMA compared to DSC.[73,74] The relatively more dramatic increase in T_g upon photo-cross-linking of the low molar mass precursors was attributed to the shorter distance between cross-link points, which leads to a higher cross-link density. On the other hand, the lower T_gs obtained for networks based on higher molar mass precursors is consistent with less cross-link density due to larger distance between cross-link points.[39]

Mechanical Analysis. The tensile properties of the photo-cross-linked films, which were evaluated according to ASTM Standard D3368, strongly depended on precursor composition and corresponding molar mass (Table 3). The PDLLA-UM networks that are capable of hydrogen bonding were relatively more rigid and had higher tensile strengths and moduli, while relatively low tensile properties were obtained for the PDLLA-M networks that were incapable of urethane hydrogen bonding. The tensile strength (TS) of the low molar mass PDLLA-M (2.9K) was 8 ± 1 MPa, while the stress-at-break of a nearly equivalent, molar mass PDLLA-UM network (2.3K) was significantly higher at 21 ± 3 MPa.

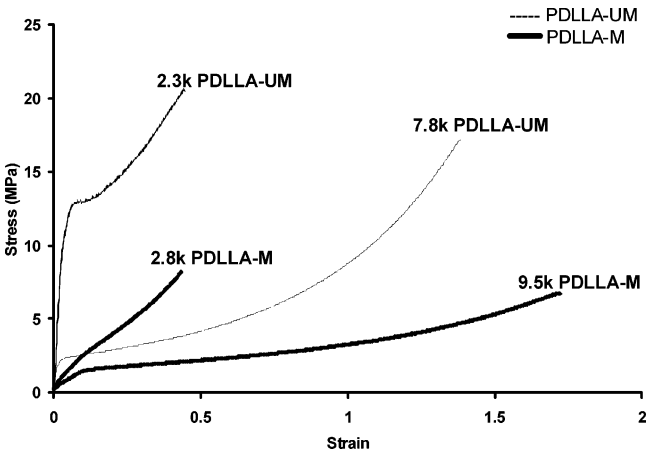

Figure 5. Stress−strain curves for PDLLA-M and PDLLA-UM, which depict the influence of urethane hydrogen bonding on the network performance.

Similar results were obtained for the networks based on high molar mass precursors. The PDLLA-UM film (7.8K) possessed a TS of 17 ± 3 MPa compared with 7 ± 3 MPa for the PDLLA-M film (9.5K). Moreover, the hydrogen-bonding urethane site significantly contributed to the Young's modulus of the networks, with the PDLLA-UM possessing tensile moduli of 113−354 MPa, which is an order of magnitude higher than those observed for PDLLA-M samples (12−21 MPa). The elongation-at-break of the network films based on the high molar mass precursors ranged from 138% to 172%, while the low molar mass precursors were approximately 44%. Distinct yield points were observed for the PDLLA-UM networks, which were capable of hydrogen-bonding interactions, while the PDLLA-M networks did not exhibit yield points. These results are consistent with the disruption of hydrogen-bonding interactions in the PDLLA-UM networks.[75] The network from the lower molar mass PDLLA-UM precursor exhibited a significant yield point due the presence of a higher concentration of hydrogen-bonding groups. This resulted in enhanced hydrogen-bonding interactions leading to a stiffer network and, as a consequence, a well-defined yield point (Figure 5).

PDLLA−PEG−PDLLA triblock copolymer telechelic diacrylates were prepared and demonstrated to be efficient adhesives to rat medial palmar digital artery and horse vein. Preliminary evidence included sufficient burst pressures upon the addition of water to the adhered interface, and rupture of the adhered interface was not observed at moderate pressures. Additionally, there was no noticeable tissue degradation. Thus, it is expected that these urethane-containing star-shaped PEG−PDLLA multiphase systems will exhibit even higher adhesive performance due to the presence of adjacent hydrogen-bonding sites. The hydrolytic degradation of these potential bioadhesives is currently under investigation in our laboratories. Future efforts will involve the evaluation of cytotoxicity and in vitro tissue testing.

Conclusions

Low T_g four-arm, star-shaped, PDLLAs of controlled molar mass, ranging from 1500 to 9500 g/mol, and narrow molar mass distribution (1.06−1.20) were prepared by use

of an ethoxylated pentaerythritol initiator for the ring-opening polymerization of DLLA. Functionalization of the PDLLA oligomers with MAAH yielded PDLLA-M with conversions ranging from 90% to 98%, while quantitative functionalization was obtained when the PDLLA oligomers were reacted with IEM to yield PDLLA-UM. In situ FTIR spectroscopy was used to monitor the formation of PDLLA-UM and showed the complete consumption of the PDLLA hydroxyl end groups and the concurrent formation of the urethane carbonyl in less than 1 h. Subsequent photo-cross-linking of the PDLLA-M and PDLLA-UM precursors resulted in highly cross-linked networks with gel contents ranging from 90% to 99%. Dramatic increases in T_gs were observed for low molar mass networks compared to their higher molar mass counterparts. Additionally, networks that were based on low molar mass oligomers were generally more rigid, while those based on higher molar mass precursors exhibited higher elongation. Tensile strengths (TS) of the low and higher molar mass PDLLA-M samples were 8 ± 1 and 7 ± 3 MPa, respectively, while the Young's moduli were 21 ± 10 and 12 ± 4 MPa, respectively. The presence of a urethane segment in the PDLLA-UM samples significantly increased the TS and Young's modulus. Low molar mass PDLLA-UM samples exhibited TS of 21 ± 3 MPa and Young's modulus of 354 ± 42 Pa, while TS of 17 ± 3 and Young's modulus of 113 ± 13 MPa were observed for the higher molar mass PDLLA-UM network.

Acknowledgment. We thank Ms. Ann Fornof for assistance with size-exclusion chromatography, Dr. Taigyoo Park for assistance with dynamic mechanical analysis, Professor Iskender Yilgor (Koc University, Turkey) for technical discussions, and Dr. Cheryl Heisey for manuscript review. This material is based upon work supported by the U.S. Army Research Laboratory and the U.S. Army Research Office under Contract/Grant DAAD19-02-1-0275, Macromolecular Architecture for Performance Multidisciplinary University Research Initiative (MAP MURI). We also acknowledge Nanosonic Inc. for complementary funding of lactide-based block copolymer studies.

References and Notes

(1) Wang, F.; Lee, T.; Wang, C.-H. *Biomaterials* **2002**, *23*, 3555.
(2) Hagan, S. A.; Coombes, A. G. A.; Garnett, M. C.; Dunn, S. E.; Davis, M. C.; Illum, L.; Davis, S. S.; Harding, S. E.; Purkiss, S.; Gellert, P. R. *Langmuir* **1996**, *12*, 2153-2161.
(3) Ertl, B.; Heigl, F.; Wirth, M.; Gabor, F. *J. Drug Targeting* **2000**, *8*, 173−184.
(4) Rimpler, M. *Int. J. Adhes. Adhes.* **1996**, *16*, 17−20.
(5) Garcia, P. J. M.; Jorge, H. E.; Millan, I.; Rocha, A.; Maestro, M.; Castillo-Olivares, J. L.; Carrera, S. A.; Cordon, A. S. *J. Biomater. Appl.* **2004**, *18*, 179−192.
(6) Nomori, H.; Horio, H.; Suemasu, K. *Surg. Today* **2000**, *30*, 244−248.
(7) Sung, H. W.; Huang, D. M.; Chang, W. H.; Huang, R. N.; Hsu, J. C. *J. Biomed. Mater. Res.* **1999**, *46*, 520−530.
(8) Sung, H. W.; Huang, D. M.; Chang, W. H.; Huang, L. L. H.; Tsai, C. C.; Liang, I. L. *J. Biomater. Sci.: Polym. Ed.* **1999**, *10*, 751−771.
(9) Flahiff, C.; Feldman, D.; Saltz, R.; Huang, S. *J. Biomed. Mater. Res.* **1992**, *26*, 481−491.
(10) Orr, T. E.; Patel, A. M.; Wong, B.; Hatzigiannis, G. P.; Minas, T.; Spector, M. *J. Biomed. Mater. Res.* **1999**, *44*, 308−313.
(11) Ninan, L.; Monahan, J.; Stroshine, R. L.; Wilker, J. J.; Shi, R. *Biomaterials* **2003**, *24*, 4091−4099.
(12) Chivers, R. A.; Wolowacz, R. G. *Int. J. Adhes. Adhes.* **1997**, *17*, 127−132.
(13) Khowassah, M. A.; Shippy, R. L. *J. Biomed. Mater. Res.* **1971**, *5*, 159−168.
(14) Park, D. H.; Kim, S. B.; Ahn, K. D.; Kim, E. Y.; Kim, Y. J.; Han, D. K. *J. Appl. Polym. Sci.* **2003**, *89*, 3272−3278.
(15) Papatheofanis, F. J. *J. Biomed. Mater. Res.* **1989**, *23*, 661−668.
(16) Samson, D.; Marshall, D. *Neurosurgery* **1986**, *65*, 571−572.
(17) Tseng, Y. C.; Tabata, Y. T.; Hyon, S. H.; Ikada, Y. *J. Biomed. Mater. Res.* **1990**, *24*, 1355.
(18) Albes, J. M.; Krettek, C.; Hausen, B.; Rohde, R.; Haverich, A.; Borst, H. G. *Ann. Thorac. Surg.* **1993**, *56*, 910.
(19) Siedentop, K. H.; Park, J. J.; Sanchez, B. *Arch. Otolaryngol. Head Neck Surg.* **1995**, *121*, 769.
(20) Kirsch, A. J.; Duckett, J. W.; Snyder, H. M.; Canning, D. A.; Harshow, D. W.; Howard, P.; Makarak, E. J.; Zderic, S. A. *Urology* **1997**, *50*, 263−272.
(21) Poppas, D. P.; Massicotte, J. M.; Stewart, R. B.; Roberts, A. B.; Atala, A.; Retik, A. B.; Freeman, M. R. *Lasers Surg. Med.* **1996**, *19*, 360−368.
(22) Aoki, H.; Tetsushi, T.; Hirofumi, S.; Hisatoshi, K.; Kazunori, K.; Tanaka, J. *Mater. Sci. Eng. C* **2004**, *24*, 787−790.
(23) Lando, G.; Cohn, D. *J. Mater. Sci: Mater. Med.* **2003**, *14*, 181−186.
(24) Cohn, D.; Lando, G. *Biomaterials* **2004**, *25*, 5875−5884.
(25) Huang, K.; Lee, B. P.; Ingram, D. R.; Messersmith, P. B. *Biomacromolecules* **2002**, *3*, 397−406.
(26) Mo, X.; Iwata, H.; Matsuda, S.; Ikada, Y. *J. Biomater. Sci.: Polym. Ed.* **2000**, *11*, 341−351.
(27) Hoffman, G. T.; Soller, E. C.; McNally-Heintzelman, K. M. *Biomed. Sci. Instrum.* **2002**, *38*, 53−58.
(28) Riley, J. N.; Dickson, T. J.; Hou, D. M.; Rogers, P.; March, K. L. *Biomed. Sci. Instrum.* **2001**, *37*, 451−456.
(29) Sorg, B. S.; Welch, A. J. *Proc.SPIE-Int. Soc. Opt. Eng.* **2001**, *4244*, 180−188.
(30) Sorg, B. S.; Welch, A. J. *Lasers Surg. Med.* **2002**, *31*, 339−342.
(31) Soller, E. C.; Hoffman, G. T.; McNally-Heintzelman, K. M. *Biomed. Sci. Instrum.* **2003**, *39*, 18−23.
(32) Kao, F.; Manivannan, G.; Sawan, S. P. *J. Biomed. Mater. Res.* **1997**, *38*, 191−196.
(33) Kim, B. S.; Hrkach, J. S.; Langer, R. *Biomaterials* **2000**, *21*, 259−265.
(34) Ono, K.; Saito, Y.; Yura, H.; Ishikawa, K.; Kurita, A.; Akaike, T.; Ishihara, M. *J. Biomed. Mater. Res.* **2000**, *49*, 289−295.
(35) Nakayama, Y.; Matsuda, T. *J. Biomed. Mater. Res.* **1999**, *48*, 511−521.
(36) Okino, H.; Manabe, T.; Tanaka, M.; Matsuda, T. *J. Biomed. Mater. Res. Part A* **2003**, *66A*, 643−651.
(37) Trenor, S. R.; Long, T.; Love, B. J. *Macromol. Chem. Phys.* **2004**, *205*, 715−723.
(38) Lang, M.; Chu, C.-C. *J. Appl. Polym. Sci.* **2002**, *86*, 2296.
(39) Helminen, A. O.; Korhonen, H.; Seppala, J. V. *J. Appl. Polym. Sci.* **2002**, *86*, 3616−3624.
(40) Ryner, M.; Valre, A.; Albertsson, A.-C. *J. Polym. Sci. Part A: Polym. Chem.* **2002**, *40*, 2049−2054.
(41) Matsuda, T.; Kwon, I.; Kidoaki, S. *Biomacromolecules* **2004**, *5*, 295−305.
(42) Bigg, D. M. *Adv. Polym. Technol.* **2005**, *24*, 69−82.
(43) Hao, J.; Whitaker, M. J.; Wong, B.; Serhatkulu, G.; Shakesheff, K. M.; Howdle, S. M. *J. Pharm. Sci.* **2004**, *93*, 1083−1090.
(44) Ouchi, T.; Kontani, T.; Ohya, Y. *Polymer* **2003**, *44*, 3927−3933.
(45) Tsuji, H.; Ikada, Y. *J. Appl. Polym. Sci.* **1996**, *60*, 2367−2375.
(46) Frick, M. E.; Zalusky, A. S.; Hillmyer, M. A. *Biomacromolecules* **2003**, *4*, 216−223.
(47) Pluta, M. *Polymer* **2004**, *45*, 8239−8251.
(48) Paul, M.; Alexandre, M.; Degee, P.; Henrist, C.; Rulmont, A.; Dubois, P. *Polymer* **2002**, *44*, 443−450.
(49) Nijenhuis, A. J.; Colstee, E.; Grijpma, D. W.; Pennings, A. J. *Polymer* **1996**, *37*, 5849.
(50) Sheth, M.; Kumar, R. A.; Dave, V.; Gross, R. A.; Mccarthy, S. P. *J. Appl. Polym. Sci.* **1997**, *66*, 1495−1505.
(51) Bechtold, K.; Hillmyer, M. A.; Tolman, W. B. *Macromolecules* **2001**, *34*, 8641−8648.
(52) Yamauchi, K.; Lizotte, J. R.; Long, T. E. *Macromolecules* **2002**, *35*, 8745−8750.
(53) Yamauchi, K.; Lizotte, J. R.; Long, T. E. *Macromolecules 36*, 1083−1088.
(54) McKee, M. G.; Elkins, C. L.; Long, T. E. *Polymer* **2004**, *45*, 8705−8715.

(55) Mather, B. D.; Lizotte, J. R.; Long, T. E. *Macromolecules* **2004**, *37*, 9331−9337.
(56) Elkins, C. L.; Yamauchi, K.; Long, T. E. *Polym. Prepr. (Am. Chem. Soc., Div. Polym. Chem.)* **2003**, *44*, 576−577.
(57) Yilgor, I.; Mather, B. D.; Unal, S.; Yilgor, E.; Long, T. E. *Polymer* **2004**, *45*, 5829−5836.
(58) Pasquale, A. J.; Long, T. E. *J. Appl. Polym. Sci.* **2004**, *92*, 3240−3246.
(59) Lizotte, J. R.; Long, T. E. *Macromol. Chem. Phys.* **2004**, *205*, 692−698.
(60) Pasquale, A. J.; Fornof, A. R.; Long, T. E. *Macromol. Chem. Phys.* **2004**, *205*, 621−627.
(61) Lizotte, J. R.; Erwin, B. M.; Colby, R. H.; Long, T. E. *J. Polym. Sci. Part A: Polym. Chem.* **2002**, *40*, 583−590.
(62) Pasquale, A. J.; Allen, R. D.; Long, T. E. *Macromolecules* **2001**, *34*, 8064−8071.
(63) Williamson, D. T.; Elman, J. F.; Madison, P. H.; Pasquale, A. J.; Long, T. E. *Macromolecules* **2001**, *34*, 2108−2114.
(64) Kricheldorf, H. R.; Fechner, B. *Biomacromolecules* **2002**, *3*, 691−695.
(65) Kricheldorf, H. R.; Fechner, B. *J. Polym. Sci. Part A: Polym. Chem.* **2002**, *40*, 1047−1057.
(66) Finne, A.; Albertsson, A.-C. *Biomacromolecules* **2002**, *3*, 684−690.
(67) Dobrzynski, P.; Li, S.; Kasperczyk, J.; Bero, M.; Gasc, F.; Vert, M. *Biomacromolecules* **2005**, *6*, 483−488.
(68) Kricheldorf, H. R.; Boettcher, C.; Toennes, K. U. *Polymer* **1992**, *33*, 2817−2824.
(69) Hsu, S.; Lin, Z. *Colloids Surf. B.* **2004**, *36*, 1−12.
(70) Aldenhoff, Y. B. J.; Van der Veen, F. H.; ter Woorst, J.; Habets, J.; Poole-Warren, L. A.; Koole, L. H. *J. Biomed. Mater. Res.* **2000**, *54*, 224−233.
(71) Lin-Gibson, S.; Bencherif, S.; Cooper, J. A.; Wetzel, S. J.; Antonucci, J. M.; Vogel, B. M.; Horkay, F.; Washburn, N. R. *Biomacromolecules* **2004**, *5*, 1280−1287.
(72) Yilgor, I.; Mather, B. D.; Unal, S.; Yilgor, E.; Long, T. E. *Polymer* **2004**, *45*, 5829−5836.
(73) Cantor, S. A. *J. Appl. Polym. Sci.* **2000**, *77*, 826−832.
(74) Margaritis, A. G.; Kalfoglou, N. K. *Polymer* **1987**, *28*, 497−502.
(75) Yang, W.; Shen, J.; Zhu, S.; Chang, C. *J. Appl. Polym. Sci.* **1998**, *67*, 2035−2045.

BM050375I